Real-Time Parameter Setpoint Optimization for Electro-Hydraulic Traction Control Systems

Addison Alexander and Andrea Vacca

Mechanical Engineering, Purdue University, West Lafayette, IN USA
E-mail: addisonalexander@purdue.edu, avacca@purdue.edu

Abstract

Many modern off-road construction machines incorporate traction control systems to provide better performance and stability in harsh driving conditions. These systems are capable of controlling wheel slip in such a way that the tractive force is increased, tire consumption is reduced, and the overall safety of the machine is improved. However, the driving surface conditions can have a strong impact on the optimal control parameters for the traction control system. This paper sets forth a method of automatically tuning the controller parameters in real time, so that the system can maximize the tractive force on its own.

Toward this end, a simple longitudinal wheel dynamics model is developed using a construction machine as a reference. This model incorporates considerations for the generation of tire force, wheel slip dynamics and machine transmission. Then, a simple traction control structure using proportional-integral-derivative (PID) control is presented which attempts to keep the machine wheels from slipping excessively. Finally, a real-time optimization scheme using the extremum-seeking algorithm was included in the system in order to automatically improve the setpoint of the controller by maximizing the pushing force of the machine. Using the vehicle model of the system, the auto-tuning controller is tested to determine the capability of the system to improve the performance. The optimization scheme allows the controller to find the optimal point, meaning that the output force can be increased when starting at a poor setpoint. Given the availability of a proper feedback signal, this system should be widely applicable to a wide range of different vehicle systems for incorporating traction control.

Keywords: Traction control, electro-hydraulic braking, optimization, automatic parameter tuning

1 Introduction

Traction control systems have become standard components in on-road vehicle systems over the past decades. Other industries such as heavy construction machinery have not seen such a strong proliferation of these systems, though there are some examples of traction control in commercially available construction machines [1]–[3]. The benefits gained by achieving a proper control of a vehicle's tires are well documented, and they include reduced tire consumption, increased traction force and increased vehicle drivability and safety. Therefore, it is desired to design an appropriate traction control system for use with construction equipment.

While the previous efforts listed above toward traction control for construction machines have been successful in reducing slip in certain operating conditions, little effort has been documented in literature in the direction of systems which can adjust to actually improve the traction control as conditions change. This paper describes the structure of an automatically-tuned controller for an electro-hydraulic braking system that reduces wheel slippages by acting on the wheel brakes. In the case of excessive torque from the transmission system causing slip at one wheel, the controller applies a proper braking torque to set the wheel at an optimum slip condition. The vehicle considered as a reference is a wheel loader (fig. 1).

One of the most difficult aspects of designing a traction controller is determining the setpoint for the control signal. Construction machines present a very particular set of problems, due to the unpredictable rapid changes in the operating conditions and diving surfaces used. Because of this, the controller parameters have to be able to quickly adapt to different conditions to avoid poor performance.

Therefore, this work focuses on devising a strategy for updating the controller parameters of the traction control system in real time so that the controller can function in the best possible condition on all surfaces. To do that, a simple traction control system has been designed and simulated to determine the effectiveness of the auto-tuning control approach.

In order to determine the effectiveness of a potential traction control strategy on the reference machine, a simulation model was created using standard vehicle dynamics formulations.

This model was then run using a simple feedback control structure to actuate the brakes in order to reduce the occurrence of excessive wheel slip. The simulation model incorporates both the dynamics of the machine itself and its wheels, as well as a model of the tire-road surface interaction and generated forces at each wheel.

This paper sets forth the outline of such a self-tuning controller. First, the dynamic system model is described, taking into account both vehicle dynamics and tire force generation. Next, a simple but effective control structure is developed which can keep the machine wheels from slipping beyond a desired value. Then, the ES optimization algorithm is incorporated into the model alongside the traction controller. Finally, a simulation is run using the simulation model which shows the performance capability of the system and the usefulness of incorporating the optimization structure into the control structure.

Figure 1: Reference vehicle and setup for testing traction control.

2 State of the Art

Many different methods have been developed for modeling the dynamic behavior of vehicles. The overall vehicle dynamics model incorporated into this work is based on models like those in Gillespie [4], Jazar [5], and Rajamani [6]. For considering the traction at the tire-road interface, a more specific model is needed. For this study, the slip-friction relationship of the tire-surface interface is modeled using Pacejka's Magic Formula tire model [7]. This is a semi-empirical tire friction model which fits a curve of values with particular characteristics to a data set.

Next, a simple traction control structure for maintaining wheel traction was developed. This control structure attempts to increase tractive force and decrease tire slip by actuating the system brakes. There are numerous different traction control strategies which have previously been developed for various different vehicle systems. Often these strategies are constructed in order to overcome specific limitations within the system. It is very common to incorporate structures such as sliding-mode control, adaptive controllers, and fuzzy logic into the designed controls for these systems [8], [9]. Due to the uncertain nature of the various system parameters, tools like state estimators are also frequently utilized in these systems [10], [11]. For this work, instead, a self-tuning proportional-integral-derivative (PID) control was formulated. This controller can be incorporated well into many different systems. The optimization aspect of this controller allows it to account for model complexities such as the transmission system effects without requiring a complicated model-based control structure.

After selecting the PID controller structure, the actual parameters to be used must be determined. In particular, the wheel slip setpoint for the controller can have a strong impact on the system performance. Depending on the ground condition, the optimal setpoint can change quite a bit, and a poor setpoint will not allow the system to reach its maximum possible tractive force. Furthermore, because of the complex interactions of the different system components, if the wheels are on different ground conditions, the restrictions given by the transmission system can make determining the optimal setpoint for all four wheels rather difficult. Therefore, an optimization technique was employed to tune the controller setpoint automatically.

Due to the well-conditioned behavior of the slip-friction relationship, several different optimization techniques could be used for this system. For the purposes of this work, the optimization method selected is the extremum-seeking (ES) algorithm. The ES algorithm has been shown to be useful for real-time optimization of dynamic systems [12]. This method has previously been used by the authors' research team for other real-time optimization applications, specifically with regard to vibration reduction in a mobile crane [13], [14]. Having constructed the full system including an optimization strategy, it can be simulated in order to determine its capability to find the maximum tractive force.

3 Vehicle Dynamics

In order to determine the capability of the traction control system, it must be simulated using a sufficiently accurate model of the machine dynamics. The vehicle model needs to account for the motion of both the chassis and the wheels, as well as the transmission system which connects the wheels together.

It is important to note that the system model developed here considers only straight-line motion of the wheel loader. This simplification is due to the fact that the primary operational mode for implementing traction control on this system is when the machine is pushing into a work pile. In the most common loading and unloading cycles (e.g. the Y-cycle), the wheel loader approaches the work pile in a straight line and does not turn significantly until it reverses out of the pile. As this is the primary operation which will likely need significant traction control, the system model has only been developed for longitudinal motion. Should the need arise for incorporating lateral motion into the model, that can be done at a later time.

3.1 Quarter-Car Vehicle Model

Before taking into account the complete vehicle system with weight transfer and multiple interconnected wheels, the general motion of the machine and its coupling to a single wheel is developed. Essentially, this creates a system modeled as a single point mass on top of a single wheel. As the full system contains four wheels, this simplified model is known as a *quarter-car* vehicle model.

Essentially, this model takes into account the force balance on the vehicle mass and the torque balance on the wheel to describe the motion of those bodies.

$$m\dot{v}_x = F_x - F_{roll}\,\mathrm{sgn}(v_x) - F_{resist}\,\mathrm{sgn}(v_x) \qquad (1)$$

$$I_w\dot{\omega} = T_E - T_B\,\mathrm{sgn}(\omega) - r_d F_x \qquad (2)$$

In eq. (1), m represents the quarter-car vehicle mass, v_x is the longitudinal vehicle velocity, F_x is the longitudinal force produced by the tires, F_{roll} is the rolling resistance, and F_{resist} is all other resistive forces acting on the vehicle (including air resistance, etc.). Equation (2) also contains the wheel moment of inertia I_w, the wheel rotational velocity ω, the input engine torque to the wheel T_E, braking torque T_B, and the dynamic radius of the wheel r_d.

For the simulation, the inputs to the system are engine torque and braking torque. Resistive forces are typically modeled either as constants or as functions of system velocity, though there are other more complex models which can be applied [5], [6], [15]. The wheel force F_x is typically calculated as a function of wheel slip, which is discussed at length in Section 4 of this paper.

Of course, this model is overly simplistic for modeling a complete vehicle system. Therefore, it must be expanded toward a full model by including wheel dynamics equations, equivalent to eq. (2) for each wheel. This means that the full machine model will actually have five equations in total: four for the dynamics of the wheels and another for the linear motion of the vehicle chassis. However, the input to the system remains a single engine torque, so the model needs to be expanded further to account for the distribution of this torque to each wheel.

3.2 Two-Axle Vehicle Model

The next step toward developing a complete vehicle model is examining how the normal forces at each tire shift as the machine moves. As this model is only considering a wheel loader which is moving forward and backward in plane, it is assumed that the weight is balanced equally from right to left and does not shift. This is a reasonable assumption in general, since the only action being modeled for the machine is straight-line digging.

On the other hand, the forces at the front and rear axles can vary quite a lot depending on the motion of the wheel loader and outside forces acting on it. The normal forces at the front and rear axles are calculated using a force and moment balance in the plane of the wheel loader motion. This results in the following equations.

$$F_{z1} = \frac{1}{2}mg\frac{l_2}{l} - \frac{1}{2}ma_x\frac{h_{CG}}{l} - F_p\frac{h_p}{l} \qquad (3)$$

$$F_{z2} = \frac{1}{2}mg\frac{l_1}{l} + \frac{1}{2}ma_x\frac{h_{CG}}{l} + F_p\frac{h_p}{l}, \qquad (4)$$

In eq. (3) and (4), F_{z1} and F_{z2} are the normal forces at the front and rear axles, respectively. Again, these are assumed to be split equally between the right and left wheels on each axle. Calculating these forces utilizes the coefficient of gravity g, the horizontal distances from the machine center of mass to the front (l_1) and rear (l_2) wheels, the horizontal distance between the axles $l = l_1 + l_2$, the longitudinal acceleration of the vehicle a_x, the height of the center of gravity h_{CG}, the external force on the wheel loader (pile force F_p, assumed horizontal), and the height of that external force h_p.

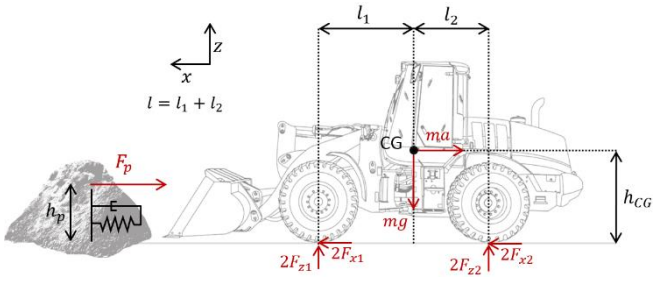

Figure 2: Wheel loader force diagram.

As the traction control system for this machine is being developed primarily for standard working conditions, the simulated operation is pushing into a work pile, which is modeled simply as a horizontal resistive force. As this work is only focused on generating excessive wheel slip and not on developing an extremely accurate digging material model, the work pile itself has been represented simply as a horizontal resistive force pushing back against the motion of the machine. The horizontal force F_p is modeled as a spring-damper system, which only acts against the motion of the machine once it has made contact.

$$F_p = \begin{cases} k_p x_p + c_p \dot{x}_p, & x_p \geq 0 \text{ and } \dot{x}_p \geq 0 \\ 0, & \text{else} \end{cases} \qquad (5)$$

In this equation, k_p and c_p are the spring and damper constants of the simulation pile, respectively, and x_p is the distance the machine has driven into the simulated pile. This allows a large resistive force to be built up quickly, but not so quickly that it causes simulation problems.

From these equations, it can be seen that, as the wheel loader accelerates forward, its weight is transferred from the front to the rear axles. Furthermore, when the machine encounters the resistive force from the pile, this also causes weight to be shifted from the front axle to the rear axle. This assumes a strictly horizontal resistive force from the pile. When digging

into a material pile, the material compaction and added weight in the machine bucket can have other effects on weight transfer which are not considered here, as they can be exceedingly complex to model properly. The changing normal force at each wheel will affect the longitudinal force that wheel is capable of producing, as the wheel force is equal to the product of the normal force and the wheel coefficient of friction (see Section 4.2).

3.3 Transmission Model

Having developed the model for transferring normal force from one axle to the other, the torque distribution to the wheels can be determined. For the wheel loader in question, this involves modeling both the front and rear differentials, which connect the driveshaft to the axles, and the transfer case, which connects the transmission to the driveshaft. It is assumed for this model that the engine torque to the driveshaft is known, so effects like the torque converter and gearbox are ignored here.

The first component of the transmission to be modeled is the differential. There are two of these in the machine linking the front and rear axles to the driveshaft. The primary purpose of the differential is to allow the wheels on each side of the axle to rotate at different velocities while still being driven by the engine. Through use of a planetary gear, the torque from the driveshaft is split in half to each wheel on the axle.

$$T_{i,L} = T_{i,R} = \frac{1}{2} R_{diff} T_{DS,i}\,, \tag{6}$$

where $T_{i,L}$ and $T_{i,R}$ are the driving torques into the left and right wheels of axle i, R_{diff} is the gear ratio of the differential, and $T_{DS,i}$ is the torque input to axle i from the driveshaft.

In order to split the torque evenly, the differential allows the wheels at each side of the axle to turn at different speeds. Of course, there is still a relationship between the driveshaft speed $\dot{\theta}_{DS,i}$ and the wheel speeds $\dot{\theta}_{L,i}$ and $\dot{\theta}_{R,i}$.

$$\dot{\theta}_{DS,i} = \frac{R_{diff}}{2}\left(\dot{\theta}_{i,L} + \dot{\theta}_{i,R}\right) \tag{7}$$

That is to say, the driveshaft speed is equal to the average of the wheel speeds on a given axle, scaled by the gear ratio.

What remains is to determine the driveshaft torque to each axle. In some vehicle systems, the driveshaft itself is driven by a central differential, splitting the torque evenly to the front and rear axles. The wheel loader in this study, however, has what is known as a *locked transfer case*, which means the front and rear section of the driveshaft are connected directly. This means that, instead of each section being able to rotate independently, they are constrained to turn at the same rate. Therefore, the torque to each axle can vary based on the load at that axle. By treating the driveshaft as a rotational mass-spring-damper system with some simplifications (as in [16]), the following equations result for describing the torque distribution to each axle.

$$T_{DS,F} = \frac{1}{2}T_E - \frac{k_{DS}}{2}\left(\theta_{DS,F} - \theta_{DS,R}\right) - \frac{c_{DS}}{2}\left(\dot{\theta}_{DS,F} - \dot{\theta}_{DS,R}\right) \tag{8}$$

$$T_{DS,R} = \frac{1}{2}T_E + \frac{k_{DS}}{2}\left(\theta_{DS,F} - \theta_{DS,R}\right) + \frac{c_{DS}}{2}\left(\dot{\theta}_{DS,F} - \dot{\theta}_{DS,R}\right) \tag{9}$$

In eq. (8(8) and (9), $T_{DS,F}$ and $T_{DS,R}$ are the torques distributed to the front and rear axles via the driveshaft, respectively, T_E is the torque into the transfer case from the engine, $\theta_{DS,F}$ and $\theta_{DS,R}$ are the angular positions of the front and rear sections of the driveshaft, respectively, and k_{DS} and c_{DS} are the rotational spring and damper constants of the driveshaft sections.

Using equations (1) through (9), the full vehicle dynamics for straight line motion have been described. Assuming a good estimate of the input torque to the transfer case and the braking torque at each wheel, this model should be appropriate for simulating the system to get an idea of controller performance.

3.4 Braking System Dynamics

A simplified schematic of the braking system designed for implementing an electronic traction control in the reference machine is shown in fig. 3 below. The traction control system uses a pressure reducing valve (1) to command a desired pressure based on the controller output. A check valve (2) is used to ensure that the higher pressure is always selected and sent to the brake caliper (3). This allows the system to operate as normal when no pressure is commanded from the traction control system, meaning that the pressure from the standard braking foot valve is seen directly by the brakes. The system is also unable to decrease the braking pressure below that of the foot valve. This is done for safety reasons, but it also means that the current system cannot implement an anti-lock brake system (ABS) or any other functionality which would require decreasing the braking pressure from the foot valve.

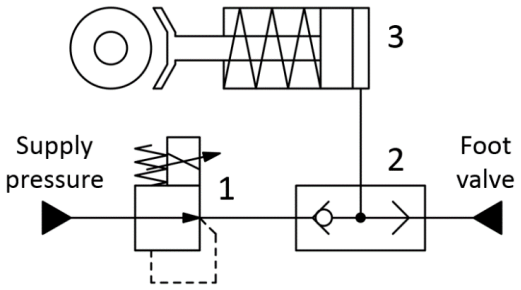

Figure 3: Simplified schematic of braking system for implementing traction control.

The modeling of this system, including valves and other braking system components like lines and shuttle valves, was accomplished using the Simscape library in Matlab Simulink. Using this library allows the simulation to account for valve dynamics, fluid compressibility, and other important hydraulic system effects. The resulting system model was then verified by comparing it with real-world system test data.

4 Tire Slip Dynamics

Where traction control is concerned, the most important component of the entire vehicle system is the interface between the tire and the road surface. This interface represents the only connection between a typical vehicle and the road, and it is also the location where the forces for propelling the vehicle are generated. Correct modeling of the interaction between a vehicle's tires and the road surface is crucial to properly modeling the vehicle system and generating an acceptable traction control structure.

4.1 Wheel Slip

Under normal operation, wheels which are being driven or braked do not rotate at a velocity which matches exactly the velocity of the road surface. In general, any time a torque is applied to the wheel deformation in the tire and other phenomena cause a small amount of slip (or micro-slip) to occur at the tire-road interface [15].

This micro-slip is different from visible slip (or macro-slip) one tends to think of when discussing wheel slip, such as spinning or sliding against the ground. In fact, micro-slip is a necessary component for force generation at the tire-road interface, as the primary force production mechanism there is friction between the tire and road surface.

Of course, it is possible to have too much slip at the tire-road interface, and in cases of excessive slip, the amount of friction force generated can decrease significantly, while also causing problems such as increased tire wear and controllability. In order to determine the effect of tire slip on tractive force, a proper model is required.

4.2 The Magic Formula Tire Model

Perhaps the most widely used model for representing the relationship between slip and force is Pacejka's Magic Formula model [7]. The Magic Formula tire model was developed as a relatively compact and simple way of representing the relationship between tire slip and the friction coefficient (i.e. tractive force) between the wheel and the road surface. It is a semi-empirical model, meaning that it is a relationship based on the general shape of slip-friction curves, which is adapted to best fit a data set for a given driving condition.

The Magic Formula is not based directly on physics equations, but it is adequate to describe the behavior of most systems. It has the form:

$$\mu_{x,i}(\kappa_i) = D_{x,i}\sin\left(C_{x,i}\tan^{-1}\left[B_{x,i}\kappa_i - E_{x,i}\left(B_{x,i}\kappa_i - \tan^{-1}\left[B_{x,i}\kappa_i\right]\right)\right]\right), \quad (10)$$

where $\mu_{x,i}$ and κ_i are the longitudinal friction coefficient and the slip ratio at wheel i, respectively. Coefficients $B_{x,i}$, $C_{x,i}$, $D_{x,i}$, and $E_{x,i}$ are parameters affecting the shape of the Magic Formula curve, and they are adjusted in order to approximate a given data set as closely as possible. The data itself can be generated through several different methods, such as the one developed by Rajamani [17].

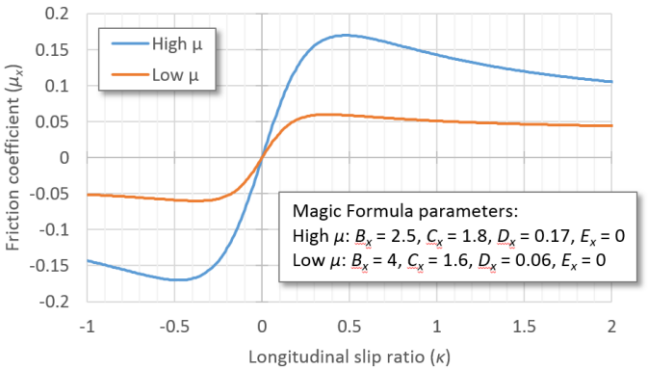

Figure 4: Example Magic Formula plots.

What results from the proper setting of the Magic Formula parameters is a plot similar to the examples shown in fig. 4. These example curves were taken from real-world test data and were used for the simulations shown in Section 7 of this work. Using the form in eq. (10), the result is an odd function. Typically, though not always, this plot has a well-defined maximum at some optimal value of κ. The objective of the traction control system is usually to keep the wheel slip at or below this value.

To convert the friction coefficient from eq. (10) to a longitudinal tractive force, it simply has to be multiplied by the normal force at that wheel.

$$F_{x,i} = \mu_{x,i}F_{N,i}\,, \quad (11)$$

where $F_{x,i}$ is the tractive force and $F_{N,i}$ is the normal force at the wheel in question. Depending on the desired accuracy of the model, the normal force can either be considered constant or it can be modeled as a time-varying force. The longitudinal force generated from eq. (11) can then be fed back into the equations of motion for the vehicle to update the linear dynamics.

4.3 Tire Slip Modeling

Since tire tire-road friction (and hence tractive force) is a function of tire slip, it is necessary to have an acceptable model for slip ratio which approximates well the behavior of the system.

In general, the tire slip model simply needs to quantify the relationship between the longitudinal motion of the vehicle and the rotational motion of each wheel. The simplest form definition of the tire slip ratio is an algebraic relationship, such as the one shown below [4].

$$\kappa_i = \frac{r_d\omega_i - v_x}{v_x} \quad (12)$$

In eq. (12), v_x represents the longitudinal velocity of the vehicle, r_d is the dynamic radius of the wheel, and ω_i is the rotational velocity of wheel i. This relationship is adequate for many modeling applications, but in some cases a more complex definition is needed. Traction control systems in

particular represent such a case, as the low velocities where they are most commonly used cause eq. (12) to vary rapidly with small variations in v_x. Furthermore, it cannot be used in the case where the vehicle stops completely ($v_x = 0$).

Therefore, a different tire slip formulation is needed which does not have such issues at low velocities. For the purposes of this research, the following definition has been defined, based on the work of Bernard [18].

$$\dot{\kappa}_i + \frac{|v_x|}{B}\kappa_i = \frac{r_d\omega_i - v_x}{B}, \qquad (13)$$

where B is the longitudinal relaxation length of the tire, and all other coefficients are the same as above. This new tire slip definition is a differential relationship, as opposed to the previous algebraic relationship. Thus, the velocities are allowed to approach and reach zero without creating the same problems.

Using eq. (13) to model the wheel slip and eq. (10) with the proper parameter values, the force generation dynamics at each tire of the vehicle can be adequately modeled.

5 Traction Control Design

A traction control system seeks to achieve relatively simple goals. First, there should be a reduction in tire macro-slip (i.e. significant visible slip against the ground surface) to reduce the amount of tire wear and increase system stability. Furthermore, this reduction in slip should also see payoffs in terms of tractive force. By maintaining better traction against the ground surface, the system is able to attain higher pushing force at each wheel. Both tire slip and pushing force are measurable quantities which can provide a numerical value to the performance increase when using the traction control.

The control structure chosen for this work is a very simple proportional-integral-derivative (PID) controller. The PID is a very common control structure with well understood design principles [19]. It is also typically well-behaved for many different kinds of systems, so it is suited quite well to the machine system considered here.

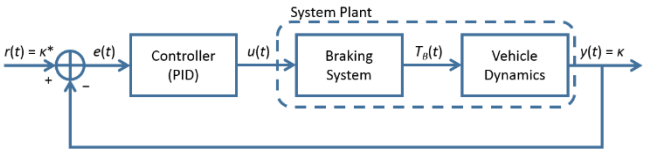

Figure 5: Overall control system block diagram.

Once the controller itself has been determined, it is important to determine how the controller should be incorporated into the overall system design. It is necessary to define an error signal from which the controller can generate the signal for the braking system. For this investigation, the control system was defined as seen in fig. 5.

From this figure, it can be seen that the feedback variable being used in this construction is the tire slips κ. Here, κ is usually a vector of slip values at all four wheels. By comparing the wheel slips to some vector of desired values κ^*, an appropriate error signal $e(t)$ is created.

One consideration which should be noted about the slip setpoint for traction control systems is that while the general controller design attempts to keep the slip *at* a certain value κ^*, in actuality the goal of the system is to keep the wheel slip *at or below* that value. As brakes are single-acting actuators, only capable of acting against the motion of the wheel, the signal itself is physically saturated in the real-world system. However, for some simulations it may be necessary to saturate the output to zero to ensure the brakes are not attempting to increase the wheel speed. The concept of brakes as single-acting inputs also plays an important role in developing the optimization algorithm in Section 6 of this work.

6 Real-Time Controller Setpoint Optimization

Having defined a proper control strategy for the traction control system, it is important to correctly set the parameters of the system for the best possible control performance. The simplest way to do this would be to pick a wheel slip setpoint which is reasonable for all wheels and allow it to remain constant. While such a setup would most likely show an improvement over no traction control system, it is also probable that a better setup can be achieved. Ideally, the controller would be able to identify the slip setpoint which maximizes traction force (see fig. 4) on its own.

6.1 The Extremum-Seeking Algorithm

For this particular work, the optimization strategy chosen is the extremum-seeking (ES) algorithm. This is a non-model-based approach which uses sinusoidal perturbations to ascertain the gradient of an objective function. The parameter or parameters to be optimized are then adjusted according to the cost function gradient to either minimize or maximize the objective function. The general continuous-time implementation of this algorithm is shown below (as formulated by Ariyur [12].

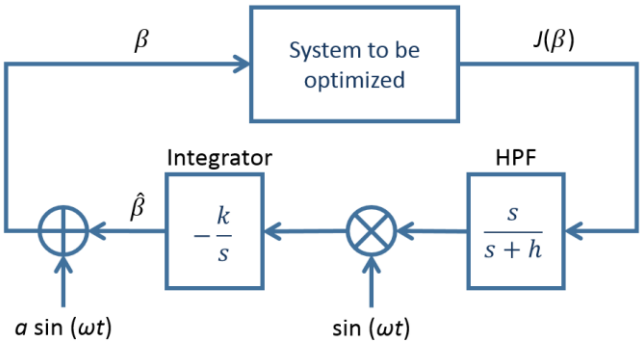

Figure 6: Basic extremum-seeking optimization scheme.

Essentially, the ES algorithm begins with an estimate of the optimal parameter value $\hat{\beta}$. By applying an additive sinusoidal perturbation to this signal, the actual parameter value β which is used in the system in question causes a response in the objective function $J(\beta)$. By passing the

resulting signal through a high-pass filter (labeled "HPF" in fig.6), "demodulating" it with using a multiplicative perturbation of the same frequency, and using an integrator to remove high-frequency components, the estimate of the optimal parameter value $\hat{\beta}$ is driven toward the actual optimal value for the system β^*.

If the objective function of the system $J(\beta)$ has a well-defined optimum J^* at β^*, the ES algorithm has been shown to converge to that value, given proper setting of the ES parameters [12]. Perhaps the most difficult aspect of implementing the ES algorithm: it introduces four new terms which must themselves be set before using the optimization strategy: ω, the frequency of the perturbation frequency, a, the additive perturbation gain, h, the high-pass filter pole, and k, the integrator gain. These parameters do add a degree of difficulty to implementing the optimization, but once they are tuned sufficiently, the algorithm can work quite well.

It should also be noted that this particular system is quite well-suited to the ES optimization technique. In general, the slip-friction characteristic of tire-road surface interfaces looks something like the plot in fig. 4. These plots are continuous, and each has a single, easily definable maximum at some slip $\kappa^* > 0$. Therefore, given proper settings for the ES algorithm, the system should be able to find the best setpoint for the controller relatively efficiently.

6.2 Integration into Controller Structure

There are multiple important parameters within the controller, including the gains K_P, K_I, and K_D for the proportional, integral, and derivative components of the control law, respectively. These can have a strong impact on the system if set incorrectly, even causing an otherwise stable system to become unstable in certain circumstances [20]. However, once set correctly within reason, small changes in other parameters, specifically the tire slip setpoint, should not cause the system to become unstable. Therefore, the controller gains were not chosen as the optimization parameters for the ES algorithm.

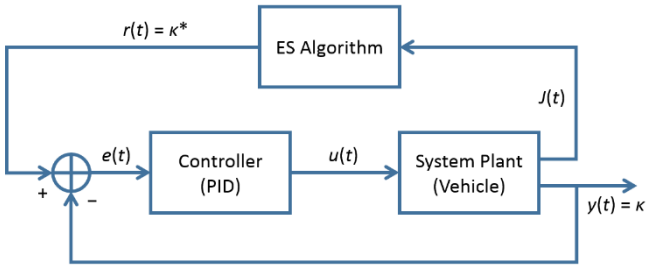

Figure 7:Control system block diagram including setpoint optimization.

Instead, the parameter to be optimized for each wheel is the tire slip setpoint. By selecting the slip setpoint instead of the controller gains, at most one value per wheel needs to be optimized, instead of potentially three or more for each wheel. This greatly simplifies the optimization process. Furthermore, the tire slip setpoint is controlled directly by the operating condition for the vehicle, so it should be a fitting parameter to use for optimizing the controller.

In order to do this, the ES algorithm must be inserted into the block diagram of fig. 5. What results is a system in which the tracking setpoint $r(t)$ is modified in real time. This reference trajectory is the equivalent of β, the output of the ES algorithm in fig. 6.

6.3 Feedback Signal Considerations

As optimization methods require a quantifiable objective function, the ES algorithm in fig. 7 receives some feedback information $J(t)$ from the system plant. The signal chosen for this feedback can have a drastic effect on the capability of the ES algorithm to optimize the controller performance.

In general, $J(t)$ needs to be chosen as a signal which quantifies the system performance in some meaningful way. For traction control systems, the primary desired output of the system is tractive force at the wheels. In standard on-road vehicle applications, the force can be approximated using the linear acceleration and wheel velocities, etc., as the vehicle is only propelling itself and is not attempting to interact with an external body [21], [22]. For construction machines like the one in question, however, the range of operating conditions and uses is significantly higher. In fact, the typical driving operation for this machine takes place at relatively low speeds, and its weight is enough that loss of traction when driving is usually not an issue.

For implementation in a real-world machine, a representative objective function needs to be constructed from available sensor data. This may not always be simple, but when specifically considering wheel loaders, a good estimate of the wheel force could potentially be generated using implement boom and bucket cylinder pressures and angles. Similar systems have already been developed for estimating the payload in the machine bucket [23], [24].

On the other hand, simulations allow for much more direct access to the system states. Therefore, the objective function for simulations can simply be the total pushing force $F_{x,tot}$ of the machine. That is,

$$J(t) = F_{x,tot} = \sum_i F_{x,i} \,. \qquad (14)$$

This objective function may be overly simplistic for some applications. For instance, Osinenko [25] includes a term for "traction efficiency," which can be included as an optimization tradeoff. Other systems may want to take into account the amount of wheel slip when creating the feedback objective function. Nevertheless, for the sake of this study, the purpose of the optimizer is simply to maximize the total pushing force of the machine.

The ES algorithm updates parameters based on the assumption that all changes in the parameters are reflected in the objective function. However, if the current braking control signal is negative, the wheel speeds are not being

affected at all. Therefore, during instances where the control signal is negative, the optimization code receives incorrect information about its effect on the system. This can cause the algorithm to converge to an incorrect point. Therefore, some logic has been added to the ES algorithm so that it does not modify the guess of κ^* unless the wheels are being braked (fig. 8). The scheme incorporating this update logic is referred to in this work as the *augmented* extremum-seeking algorithm.

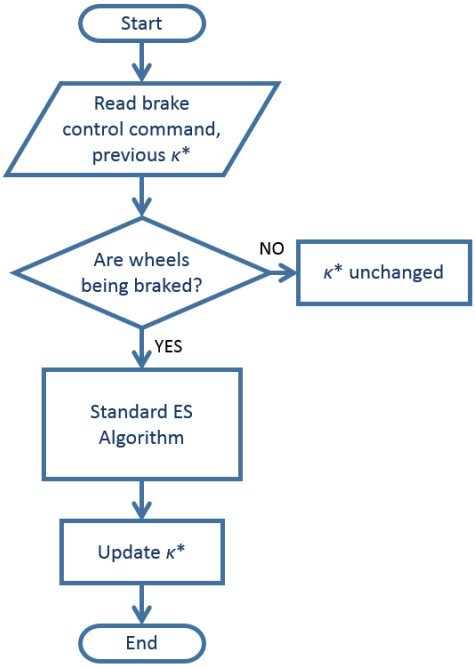

Figure 8: Augmented extremum-seeking algorithm.

7 Simulation Results

Now that the system has been properly constructed and the optimization algorithm set in place, it is necessary to determine how well the system can perform. For this work, the performance metric will be assessed using a simulation conducted in Matlab Simulink and based on the model developed in Sections 3 and 4 of this paper.

Before the traction control simulation was conducted, it was first desired to assess the accuracy of the vehicle model. This was done by running a test with a series of accelerations and braking actions and recording an estimate of the input torque to the system. This torque was then used as an input to the simulation model. The resulting simulation was compared to the results of the machine test (fig. 9).

The next simulation used for this system was a simplified digging cycle, similar to the setup shown in fig.1. In the simulation, the machine approaches the simulated pile and pushes against it for a few seconds. During that time, the controller and optimizer work together to maximize the pushing force of the machine. In theory, this increased pushing force translates, in real-world operation, to increased digging force along with decreased tire slip.

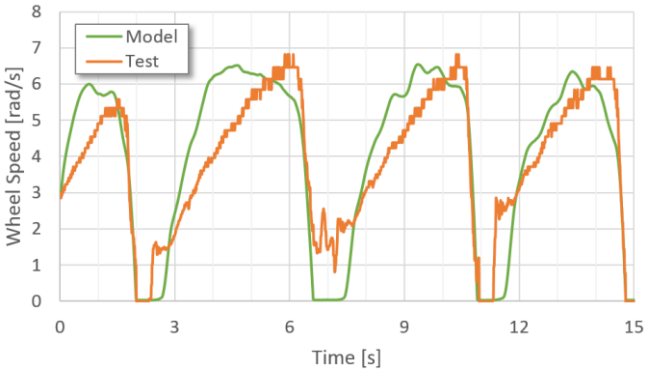

Figure 9: Simulation model validation.

For the first test, the vehicle is on a ground condition with relatively high friction for all four wheels (the high-μ example from fig. 4). The wheel loader begins the simulation by advancing toward the work pile without the wheels slipping against the ground. Once the machine reaches the pile and begins pushing against it, however, the tires begin to slip (with the vehicle velocity actually slowing down) and the tractive force is reduced. As the wheel slip increases, the traction control system activates and slows down the wheels until they are kept at the proper slip ratio. The vehicle and wheel velocities for this simulation are shown in fig. 10

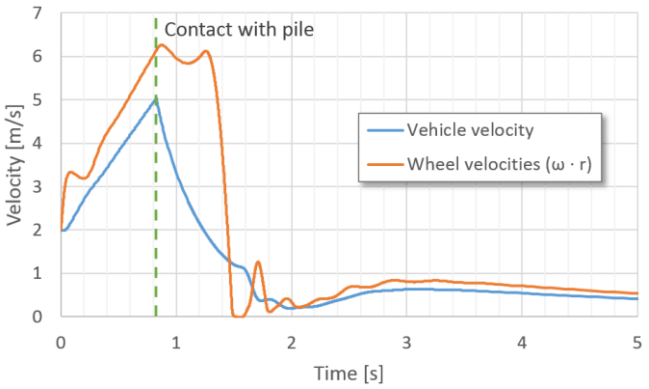

Figure 10: Traction control simulation velocities (high-friction simulation).

The overall effect of this is that the tractive force is increased and the machine can dig farther into the pile. Figure 11 shows the pushing force of the machine over time for the machine. It makes contact with the work pile after just before 1 second and quickly begins losing tractive force. As the traction control activates, at first the brakes are actuated too strongly. This causes an overshoot where the vehicle is actually slowed down for a brief moment. Very quickly, however (within two seconds), the optimization algorithm finds the correct setpoint value, and within three seconds the system has converged to a very good tractive force value. In fact, the system achieves a final force which is 54.7% higher than the final force without the traction control system (21.9 vs. 14.1 kN in this simulation). Furthermore, the wheel slip is greatly reduced in this case. This indicates that the controller is in fact meeting the requirements set for it in Section 5 of this paper. The speed at which the algorithm is able to converge

suggests that this system could be well-suited for implementation on a real-world machine.

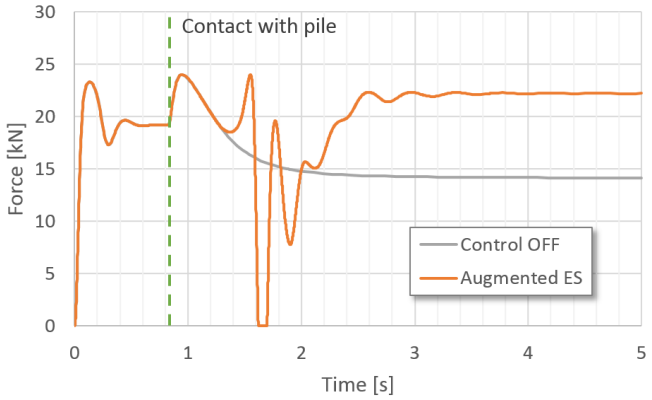

Figure 11: Longitudinal force for vehicle simulation in high-friction condition.

Figure 12 shows the result of the setpoint optimization for this simulation using the augmented extremum-seeking algorithm, as well as a comparison to the same simulation using an unmodified ES algorithm (i.e. exactly as shown in fig. 6). The tire-road interface has a known maximum friction coefficient at a slip ratio of around $\kappa^* = 0.5$. This is found by determining the location of the maximum friction coefficient for the slip friction curve, shown in fig. 4. To determine the location of the slip that maximizes the friction, the curve is differentiated with respect to κ, and then the location where the derivative curve crosses zero is taken as κ^*.

It can be seen that, even when the system is not being braked, the unmodified ES algorithm still attempts to use the force information to update the setpoint. As a result, it ends up overshooting the actual optimum value and, as the force continues to change, it could potentially wander farther from the correct point. If, on the other hand, the optimization is updated only when the brakes are being actuated (as in the augmented ES algorithm), the optimization avoids the effect of bad objective function information. Therefore, instead of the haphazard development of the standard ES algorithm, the updated ES algorithm pauses when no wheels are being braked and consistently approaches the correct setpoint as time progresses.

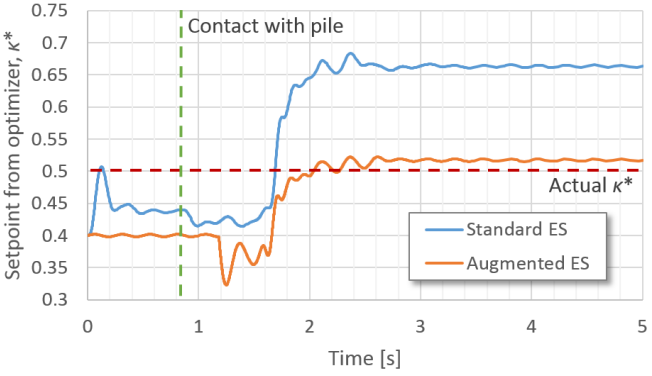

Figure 12: Performance comparison of standard ES algorithm with updated version (high-friction).

A second simulation was then run using the same system in a different ground condition. This time, all four wheels were simulated as being on slick ground (the low-μ example from fig. 4). In this condition, the traction control system must work much more to keep the wheels from spinning. Furthermore, the maximum pushing force is found at a different value of slip ratio ($\kappa^* \approx 0.36$). This means that, whereas the ES algorithm needed to increase the setpoint in the previous simulation, with this condition it must decrease the setpoint somewhat. The results of this simulation are shown in fig. 13.

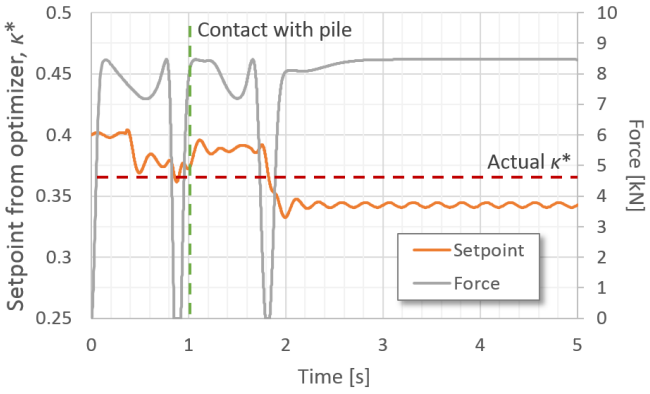

Figure 13: Simulated system performance (low-friction).

In this simulation, the controller setpoint was again initialized at a non-optimal value. In fact, it started at the same point as the high-friction simulation ($\kappa_0 = 0.4$). In this case, the ES algorithm decreased the setpoint during the simulation, so that it achieved a better setpoint. Furthermore, the traction control system was able to contain the wheel slip to an appropriate value such that the tractive force was maximized (again, after some initial overshoot where the tractive force was briefly decreased). Even in a worse ground condition, this system far outperforms a simulation with no traction control.

These simulations indicate that the system developed in this work is capable of determining and reaching an optimal slip value given the proper feedback signal for the optimization objective function.

8 System Potential

Generating the feedback signal is relatively simple in simulation, as most states can be computed fairly easily. In practice, however, it is more difficult to obtain, for instance, a proper estimate of the wheel force. Nevertheless, if an acceptable objective function can be computed, this system should be equally applicable to real-world vehicle systems. In terms of generating a longitudinal force estimate, the wheel loader presents some potential for accomplishing this. For instance, if it is being used to dig or push, the pressure in the implement boom and bucket hydraulic cylinders can be processed in such a way that a reasonable estimate of pushing force can be determined. This could potentially incorporate a system similar to the payload sensing apparatus described in [23], [24].

Nevertheless, if a suitable feedback signal can be generated, this system has quite a lot of potential toward being applicable to other systems. Using a basic PID structure for the controller means that there are very few parameters which need to be adjusted in order to apply it to a new vehicle. Other more complex model-based controllers may have somewhat better performance, but they are also very specific to the machine for which they are designed, and transferring them to other systems could require some rigorous work.

Furthermore, using the extremum-seeking algorithm also makes the controller design relatively simple to transfer to new machines. As long as the objective function is well-behaved and has a relatively well-defined maximum (or minimum), the ES algorithm is a fairly robust method for optimizing the system. Therefore, this system should be applicable toward the development of other traction control systems without very much needed modification.

9 Conclusions

This paper presents a self-tuning controller for eletro-hydraulic traction control systems in vehicles. By focusing on the case of a construction machine, a simple vehicle model is developed for simulating the performance of the traction control system. This model includes considerations for wheel force generation, including wheel slip dynamics. A relatively simple controller consisting of a PID structure was then included in order to control the wheel slip to some value.

Much work was conducted toward finding the optimal wheel slip value, which can change from one ground condition to the next. Therefore, a feedback structure was created which utilized a real-time optimization method (the extremum-seeking algorithm) in order to determine this value online. In order to do this, an objective function for the system was designated and the extremum-seeking parameters were tuned to appropriate values.

By using the automatic tuning controller, simulations were run which showed that it has the ability to determine the optimal slip value for the wheels on its own and to control the wheels to that value. This resulted in a simulation in which the wheel force was optimized in real time while pushing against a work pile (modeled as a resistive force). In all, this control structure shows promise for tuning traction control systems in vehicles which work on varied surfaces.

Nomenclature

Designation	Denotation	Unit
a_x	Longitudinal acceleration	m/s^2
B	Tire longitudinal relaxation length	m
B_x	Magic Formula parameter	none
C_x	Magic Formula parameter	none
c_{DS}	Damping rate of driveshaft section	$\frac{N \cdot m \cdot s}{rad}$
c_p	Damping rate of pile resistive force model	N·s/m
D_x	Magic Formula parameter	none
E_x	Magic Formula parameter	none
F	Force	N
g	Acceleration of gravity	m/s^2
h	High-pass filter pole for extremum-seeking algorithm	none
h_{CG}	Height of center of gravity	m
h_p	Height of pile force application	m
I_w	Wheel moment of inertia	$kg \cdot m^2$
J	Objective function value for optimization	none
k	Integral gain for extremum-seeking algorithm	none
k_{DS}	Spring rate of driveshaft section	N·m/rad
k_p	Spring rate of pile resistive force model	N/m
l	Horizontal distance	m
m	Vehicle mass	kg
R_{diff}	Gear ratio of differential	none
r	Reference trajectory for control system	none
r_d	Dynamic radius of wheel	m
T	Torque	N·m
v_x	Longitudinal vehicle velocity	m/s
x_p	Distance of travel into pile	m
β	Optimization variable(s) for extremum-seeking algorithm	none
$\hat{\beta}$	Estimate of variable optimum value for ES algorithm	none
θ	Rotational position	rad
κ_i	Slip ratio at wheel i	none
μ_x	Longitudinal friction coefficient	none
ω_i	Rotational velocity of wheel i	rad/s

References

[1] J Sjögren. "Anti spinning device, a vehicle comprising the device and a method for reducing slip during advancing of a vehicle," US 8226177 B2, 24-Jul-2012.

[2] K Uematsu, K Hatake, and A Nomura. "Vehicle speed estimator and traction control device," US 8538635 B2, 17-Sep-2013.

[3] B J Holt, J E Jensen, S Marathe, and S A Marks. “Electronic traction control system,” US 6631320 B1, 07-Oct-2003.
[4] T D Gillespie. *Fundamentals of Vehicle Dynamics*. Warrendale, PA: Society of Automotive Engineers, 1992.
[5] R N Jazar. *Vehicle Dynamics: Theory and Application*, 2nd ed. New York: Springer, 2014.
[6] R Rajamani. *Vehicle Dynamics and Control*, 2nd ed. New York, NY: Springer, 2012.
[7] H B Pacejka and E Bakker. “The Magic Formula Tyre Model.” *Vehicle System Dynamics*, 21(S1):1–18, Jan. 1992.
[8] J Li, Z Song, Z Shuai, L Xu, and M Ouyang. “Wheel Slip Control Using Sliding-Mode Technique and Maximum Transmissible Torque Estimation.” *Journal of Dynamic Systems, Measurement, and Control*, 137(11):111010, Aug. 2015.
[9] H Lee and M Tomizuka. “Adaptive Vehicle Traction Force Control for Intelligent Vehicle Highway Systems (IVHSs).” *IEEE Transactions on Industrial Electronics*, 50(1):37–47, Feb. 2003.
[10] T Nakakuki, T Shen, and K Tamura. “Adaptive control approach to uncertain longitudinal tire slip in traction control of vehicles.” *Asian Journal of Control*, 10(1):67–73, Jan. 2008.
[11] S Kuntanapreeda. “Traction Control of Electric Vehicles Using Sliding-Mode Controller with Tractive Force Observer.” *International Journal of Vehicular Technology*, 20141–9, 2014.
[12] K B Ariyur and M Krstić. *Real-Time Optimization by Extremum-Seeking Control*. Hoboken, NJ: John Wiley & Sons, Inc., 2003.
[13] D Cristofori, A Vacca, and K Ariyur. “A Novel Pressure-Feedback Based Adaptive Control Method to Damp Instabilities in Hydraulic Machines.” *SAE International Journal of Commercial Vehicles*, 5(2):586–596, Sep. 2012.
[14] G F Ritelli and A Vacca. “Energy Saving Potentials of a Novel Electro-Hydraulic Method to Reduce Oscillations in Fluid Power Machines: The Case of a Hydraulic Crane.” *SAE International Journal of Commercial Vehicles*, 6(2):269–280, Sep. 2013.
[15] H B Pacejka and I Besselink. *Tire and Vehicle Dynamics*, 3rd ed. Amsterdam: Elsevier/Butterworth-Heinemann, 2012.
[16] M M Tinker. “Wheel Loader Powertrain Modeling for Real-Time Vehicle Dynamic Simulation,” Master’s thesis, The University of Iowa, Iowa City, 2006.
[17] R Rajamani, G Phanomchoeng, D Piyabongkarn, and J Y Lew. “Algorithms for Real-Time Estimation of Individual Wheel Tire-Road Friction Coefficients.” *IEEE/ASME Transactions on Mechatronics*, 17(6):1183–1195, Dec. 2012.
[18] J E Bernard and C L Clover. “Tire Modeling for Low-Speed and High-Speed Calculations,” 1995.
[19] N S Nise. *Control Systems Engineering*, 6th ed. Hoboken, NJ: Wiley, 2011.
[20] W S Levine, Ed. *The Control Handbook*, 2nd ed. Boca Raton, Fla.: CRC Press, 2011.
[21] H Hamann, J K Hedrick, S Rhode, and F Gauterin. “Tire force estimation for a passenger vehicle with the Unscented Kalman Filter,” in *Intelligent Vehicles Symposium Proceedings*, Dearborn, MI, USA, 2014, 814–819.
[22] J Matuško, I Petrović, and N Perić. “Neural network based tire/road friction force estimation.” *Engineering Applications of Artificial Intelligence*, 21(3):442–456, Apr. 2008.
[23] H Kang, W Jung, and C Lee. “Modeling and Measurement of Payload Mass of the Wheel Loader in the Dynamic State based on Experimental Parameter Identification,” in *SAE Technical Paper 2016-01-0469*, 2016.
[24] A Shatters. “Method and system for estimating payload weight with tilt position compensation,” US 9464403 B2, 11-Oct-2016.
[25] P V Osinenko, M Geissler, and T Herlitzius. “A method of optimal traction control for farm tractors with feedback of drive torque.” *Biosystems Engineering*, 12920–33, Jan. 2015.